Faraday Discussions

Cite this: *Faraday Discuss.*, 2017, **196**, 415

View Article Online
View Journal | View Issue

PAPER

Restorable piezochromism phenomenon in an AIE molecular crystal: combined synchronous Raman scattering†

Liqun Liu,[a] Kai Wang,[b] Jian Deng,[a] Zhe Zhang,[c] Yan Wang*[c] and Yuguang Ma*[a]

Received 24th June 2016, Accepted 29th July 2016
DOI: 10.1039/c6fd00154h

Published on 29 Julai 2016. Downloaded by Fail Open on 23/07/2025 10:17:13.

Many AIE active molecules have been designed and synthesized, and have been found to possess many interesting characteristics. In recent years, research into AIE crystals has increased, and it has been clearly shown that the piezochromic effect of AIE crystals depends on their structure. While most of the related research has given qualitative results, to quantitatively reveal molecular conditions under different pressure conditions, crystals of an AIE material (2*Z*,2′*Z*)-3,3′-(1,4-phenylene)bis(2-(naphthalen-2-yl)acrylonitrile) were investigated by synchronous Raman scattering and fluorescence spectroscopies. The molecular structure of the crystal changed during the process of pressurizing and then depressurizing under hydrostatic pressure, and a 142 nm red-shift value was observed in the emission spectrum of the PBNA crystal. The crystal was transformed into a new phase when the pressure was above 1.03 GPa and returned to the original phase when the pressure was decreased. The unique restorable phase transformation process of the crystal of this AIE active material could be used for erasable optical information storage and stress sensing devices.

Introduction

In the aggregation induced emission (AIE) phenomenon, molecules which do not emit light or emit weak light in the solution state are instead able to emit strong fluorescence in the aggregated state, and this was first reported by Tang's group in 2001.[1,2] From then on, many molecules with the AIE phenomenon have been designed and synthesized, and many interesting characteristics of AIE molecules have been found.[3–13] With further research, the applications of AIE molecules

[a]*State Key Laboratory of Luminescent Materials and Devices, South China University of Technology, Guangzhou, 510640, P. R. China. E-mail: ygma@scut.edu.cn*

[b]*State Key Laboratory of Superhard Materials, Jilin University, Changchun 130012, China*

[c]*College of Chemistry, Jilin University, Changchun, 130012, P. R. China. E-mail: wangy2011@jlu.edu.cn*

† Electronic supplementary information (ESI) available: The synthetic route, HNMR IR spectra and refinement data of the crystal. CCDC 1487561. For ESI and crystallographic data in CIF or other electronic format see DOI: 10.1039/c6fd00154h

Published on 29 Julai 2016. Downloaded by Fail Open on 23/07/2025 10:17:13.

have been extended to many fields such as optoelectronics, biotechnology, sensing, medical science, *etc.*[14–17]

The chemical bonds in AIE compounds are usually flexible and easily rotated, and as a result the majority of AIE compounds have a certain response to external stimuli, such as organic solvent vapor, heat, pressure, *etc.* Recently, scientists have discovered that compounds with an AIE effect show, to a certain extent, a structural correlation with piezochromic luminescent behavior.[18–21] In order to investigate the mechanism of piezochromic photochromism, many AIE crystals with precise structures have been studied. For example, in 2010, Park's group reported an AIE-active cyano DSB derivative, DBDCS, which exerted dual-color fluorescence switching performance under pressure stimulation.[22] After careful study, they found that the molecular layers formed by intramolecular hydrogen bonding played an important role in the ability of DBDCS to produce piezochromic behavior. Meanwhile, these molecular layers have shearing and slipping abilities. Researchers have also found that molecules which stack loosely and possess holes can easily be destroyed under external force.[19–21,23] Other compounds, such as Ir(III) complexes,[24] DPDBFs[25] and some other crystals[26–28] have also been reported to prove this theory. These studies clearly show that the piezochromic effect of AIE crystals depends on their structure: AIE crystals which possess molecular layer planes can change color under pressure because the molecular layers may shear or slip.[13,22] For crystals which have a twisted non-planar structure, forming the typical π–π interaction is difficult due to the low lattice binding energy of this structure and the tendency of molecular conformation towards planarization or slipping of the molecular layers; it is easy to destroy such a structure.[23,24,26,29] Although many achievements have been made in the past few years, the relationship between pressure and the structure of AIE crystals has mainly been investigated by the method of grinding, which gives only qualitative results, not quantitative ones.[27,28]

In recent years, researchers have begun to quantitatively investigate AIE molecules, for the purpose of obtaining further understanding of the relationship between the piezochromic effect and the way molecules aggregate in the crystal.[13,26] However, the quantitative approaches are far from sufficiently elucidated, and the mechanism of pressure electroluminescence is not entirely clear. There are many in-depth physical problems requiring further research. Therefore, more effective techniques need to be utilized to reveal more about the molecular conditions at different pressures.

In this paper, an AIE material (2*Z*,2′*Z*)-3,3′-(1,4-phenylene)bis(2-(naphthalen-2-yl)acrylonitrile) (PBNA) was synthesized and its crystal was obtained. Based on the precise structure of the G phase single crystal of PBNA, the molecular structure changes during the process of adding and then releasing hydrostatic pressure were also investigated. To sufficiently analyse the structural changes during the process, synchronous Raman scattering and fluorescence spectroscopies were used. From the optical spectrum, a red-shift of 142 nm in the emission peak of the PBNA crystal was observed with the increase in pressure, and the crystal transformed into another phase when the pressure increased over 1.03 GPa. Once the pressure was reduced to less than 1.2 GPa, the new phase returned to the original one. The main breakthrough of this work is the exploration of the precise structural changes of AIE materials during the process of compressing the single crystal. By combination with the method of synchronous Raman scattering, the

 This journal is © The Royal Society of Chemistry 2017

Published on 29 Julai 2016. Downloaded by Fail Open on 23/07/2025 10:17:13.

phase transformation phenomenon in the fluorescence spectrum was certified, and this method will also aid the study of polymorphic transformations in the structures of other systems. What's more, the molecule PBNA with restorable piezochromic phase transformation characteristics under pressure could be used for the study of erasable optical information storage and stress sensing devices.

Experimental

Synthetic procedures

PBNA was synthesized and a green single crystal G was obtained *via* the sublimation growth method (shown in the ESI†). The emission spectra of PBNA were collected in water/tetrahydrofuran mixtures with different proportions, which reflected the AIE active properties (Fig. 1). When the water/tetrahydrofuran ratio is low, the molecules in solution are flexible and able to generate internal rotation, making the excitation energy attenuate in a non-radiative form, producing a weak fluorescence emission. When the water/tetrahydrofuran ratio increases to 80%, the process of molecular internal rotation is hindered and non-radiative decay is inhibited. The excitation energy attenuates in the form of radiation producing a strong fluorescence and the emission spectrum has a delicate structure. However, the luminescence intensity decreases when the ratio is 90%, because the molecules in this state aggregate much more closely, as in "H" aggregation. The AIE phenomenon also explains why PBNA crystals have a luminescence efficiency of 80%.

Single crystal structural analysis of crystal G of PBNA

The precise crystallographic structure of crystal G was elucidated using an X-ray diffractometer. Crystal G was of the typical monoclinic system, which belonged to the $C2/c$ space group. The density of the crystal was 1.267 mg m^{-3}. As shown in Fig. 2, the molecule exhibited the *trans* configuration with a torsional main

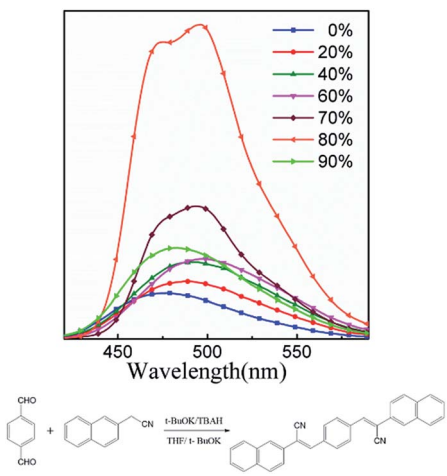

Fig. 1 Emission spectra of PBNA dissolved in water/tetrahydrofuran mixtures with different proportions and the synthetic route.

Published on 29 Julai 2016. Downloaded by Fail Open on 23/07/2025 10:17:13.

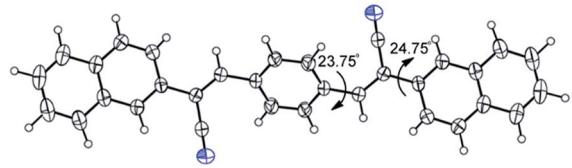

Fig. 2 The molecular conformation of PBNA in single crystal G.

carbon chain. The dihedral angle between the central benzene ring and the double bond plane was 23.75°; the one between the naphthalene ring and the plane of the double bond was 24.75°.

In the planar molecule in which the twisted angle was relatively small, the nitrogen atom of the cyano groups on both sides of the molecule interacted with the hydrogen atom on the double bond of the adjacent molecules. This interaction forced the molecules to connect constantly, forming a planar structure of π–π interactions. The length of the hydrogen bond was measured as 2.388 Å using Materials Studio, and the hydrogen bond helped the molecules to arrange in parallel and fixed the molecules in identical orientation (in Fig. 3 and 4). In Fig. 4, viewing from the *b* axis, crystal G was alternately formed by the parallel PBNA molecules, and viewing from the *c* axis, the angle between the contiguous molecular dipoles on the AOB plane was about 30° and it was foreseeable that the molecules would flatten tighter under hydrostatic pressure in all directions.

Experimental methods

Fluorescence and synchronous Raman scattering spectroscopies were used to study the molecular changes of crystal G. The Raman scattering data was collected using the micro Raman system combined with a liquid nitrogen cooled CCD (PyLon: 100B, Princeton) and a spectrometer (Acton SP2500, Princeton). The precise structure of crystal G was examined using an X-ray diffractometer and the structure data is displayed in the ESI.† The crystal was placed in symmetric diamond anvil cells (DAC) with 400 μm diamond anvils and a 150 μm gasket hole. The pressure transmission medium was a mixed methanol : ethanol solution with a volume ratio of 4 : 1 and the laser wavelength used as the excitation source was 355 nm. All of the spectra and data were collected at room temperature.

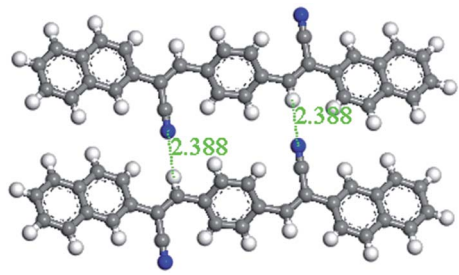

Fig. 3 Hydrogen bond in crystal G of PBNA.

Published on 29 Julai 2016. Downloaded by Fail Open on 23/07/2025 10:17:13.

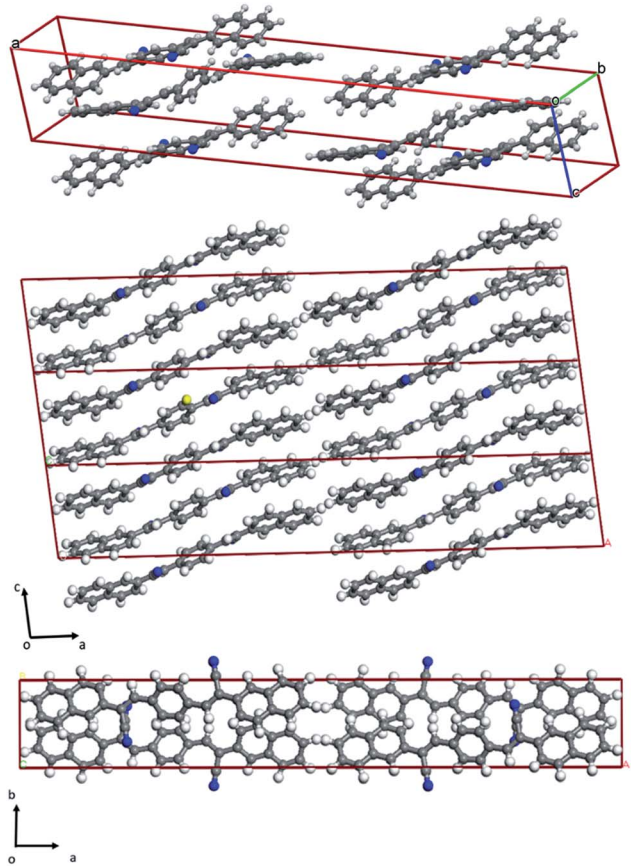

Fig. 4 Molecular arrangement in crystal G along the *b* and *c* axes.

The precise structure of crystal G was examined using an X-ray diffractometer (XRD) and a cif file illustrating the precise structure is available in the ESI.†

For the test, a piece of green crystal G was selected and set into the DAC. The emission spectrum of the crystal was collected under different hydrostatic

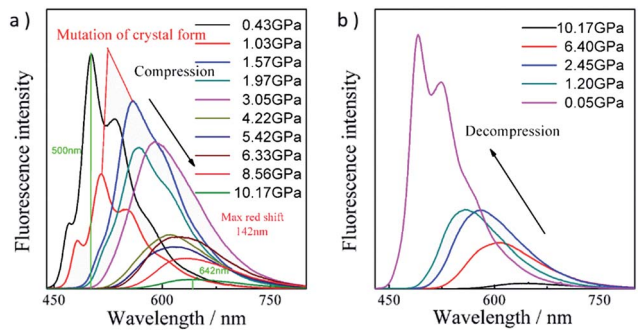

Fig. 5 Synchronous emission spectra of crystal G as a function of increasing and decreasing pressure process.

Published on 29 Julai 2016. Downloaded by Fail Open on 23/07/2025 10:17:13.

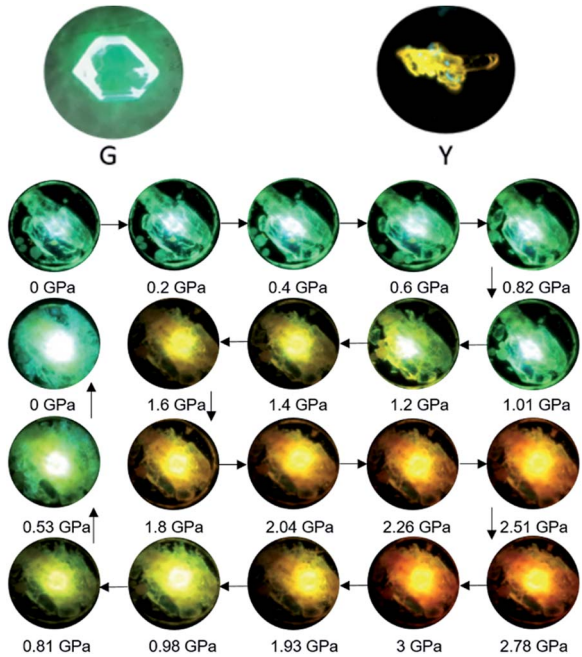

Fig. 6 Photos of the crystal's color change with increasing and then decreasing pressure.

pressure conditions (Fig. 5a). Meanwhile, pictures of crystal G at different pressures were also taken and are shown in Fig. 6.

Results and discussion

Synchronous fluorescence spectroscopy

The emission peak of crystal G was around 500 nm and the spectrum red-shifted with the increase in pressure. The largest displacement of the red-shift was 142 nm; the emission peak intensity decreased from 0 GPa to 1.57 GPa. The shape

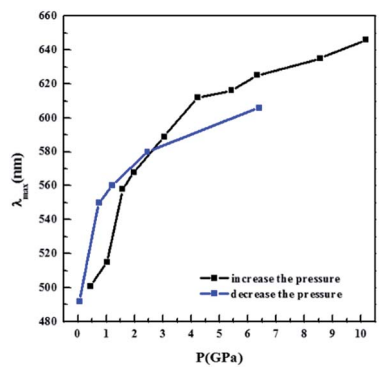

Fig. 7 The relationship between light emission peak position and pressure.

 This journal is © The Royal Society of Chemistry 2017

Published on 29 Julai 2016. Downloaded by Fail Open on 23/07/2025 10:17:13.

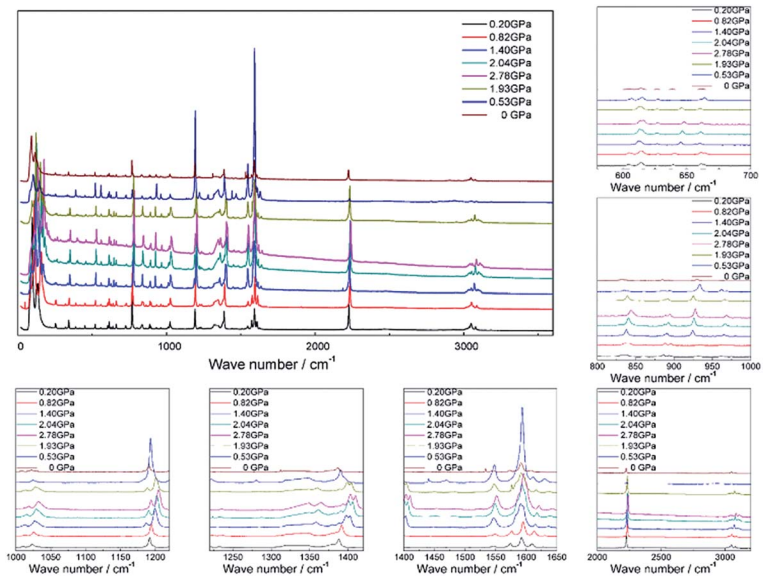

Fig. 8 Synchronous Raman spectroscopy in the crystal's piezochromic process.

of the spectrum changed and decreased as the pressure increased from 1.97 GPa to 10.17 GPa. Combining the characteristics of this material, PBNA, some factors illuminating this phenomenon are displayed as follows: (1) first, when we obtained the green phase crystal "G" of the PBNA material by the sublimation method, several small yellow phase crystals "Y" (Fig. 6) were also obtained in the same quartz tube where the temperature was lower than where crystal G grew. The quality of the "Y" phase crystal was not good enough to obtain the precise structure. Even so, this polymorphism property helped explain that the shape change of the spectrum was due to the phase transition from the "G" into the "Y" phase when crystal "G" was under increased pressure from 0 GPa to 10.17 GPa. (2) Moreover, when crystal "G" was compressed from 0.43 GPa to 1.03 GPa, the surrounding pressure compressed the molecules together tighter and the dipoles had the tendency to be totally parallel, which shortly reduced the luminous intensity. (3) Besides, when the pressure continued to be increased to a critical value, the molecules were tight enough to undergo a phase transition process. When the pressure was increased from 1.03 to 1.57 GPa, the structure of the "G" phase crystal changed a lot and obviously the luminous mechanism also changed, therefore the intensity of the new "Y" phase crystal at 1.57 GPa being higher than that at 1.03 GPa was also reasonable. (4) Next, on gradually increasing the pressure value from 1.57 GPa to 10.17 GPa, the spectrum retained a single peak shape and the spectrum intensity decreased due to the tighter structure trend and the shorter intermolecular distance. Under extremely high pressure, the crystal molecules were arranged just like a large π bond structure.

A decreased in pressure from 10.17 GPa to 0.05 GPa was sequentially applied to the same crystal G. The spectral performance was exactly the opposite of the pressurizing process: the emission spectrum of the crystal was blue-shifted as the pressure decreased. The decompression process spectra and photographs are

Published on 29 Julai 2016. Downloaded by Fail Open on 23/07/2025 10:17:13.

Table 1 Raman peak changes of crystal G and the corresponding functional groups

(Pre-compression) wave number/cm^{-1}	(Post-compression) wave number/cm^{-1}	Corresponding functional groups
3080	3109	Aromatic C–H stretch
3048	3083	Aromatic C–H stretch
2227	2241	C≡N stretch
1626	1642	C=C stretch
1608	1621	C=C stretch
1592	1596	C=C stretch
1572	1597	Symmetrical C=C stretch
1547	1551	C=C stretch
—	1483	Symmetrical C=C stretch
—	1449	N≡N stretch
1389	1410	Naphthalene
1378	1402	Naphthalene
1327–1347	1348/1364	C–H deformation
—	1290	C–H deformation
1220/1231	1236/1248	*para* disubstituted benzene stretch
1191	1193/1204	C_6H_5–C vibration
1022	1032	Mono substituted benzene inner surface C–H deformation
1010	1019	Mono substituted benzene triangle ring "breathing"
960	980	Olefin C–H vibration
930	932	C–H bend
896	897	C–C backbone stretch
885	889	C–C backbone stretch
826–838	843	*para* disubstituted benzene vibration
639	645	Mono substituted benzene vibration

shown in Fig. 5b and 6. In the decompression process, the spectrum maintained a single peak shape and the spectral intensity increased with the pressure decrease from 10.17 GPa to 1.20 GPa. The degree of molecular binding was getting smaller and molecular motion was more flexible.

When the pressure was decreased from 1.2 GPa to 0.05 GPa, the peak shape and intensity of the emission spectrum still indicated a mutation from the original state. Under reduced pressure, the pressurized crystal could be restored to the green phase, so the above process of a restorable piezochromic phenomenon was completely reversible.

The relationship between the maximum wavelength emission peak and the pressure applied during the process of pressurizing and depressurizing was also analyzed (Fig. 7). The two lines had overlapping positions; this showed that the peak location could be restored to its original position to some degree when the applied pressure was decreased to zero.

Synchronous Raman scattering spectroscopy

The piezochromic phenomenon of the crystal was then studied by synchronous Raman spectroscopy. The test range of the Raman spectroscopy was from 0 cm^{-1} to 3500 cm^{-1} (Fig. 8). In the Raman spectrum of the unpressurized crystal, the

 This journal is © The Royal Society of Chemistry 2017

Published on 29 Julai 2016. Downloaded by Fail Open on 23/07/2025 10:17:13.

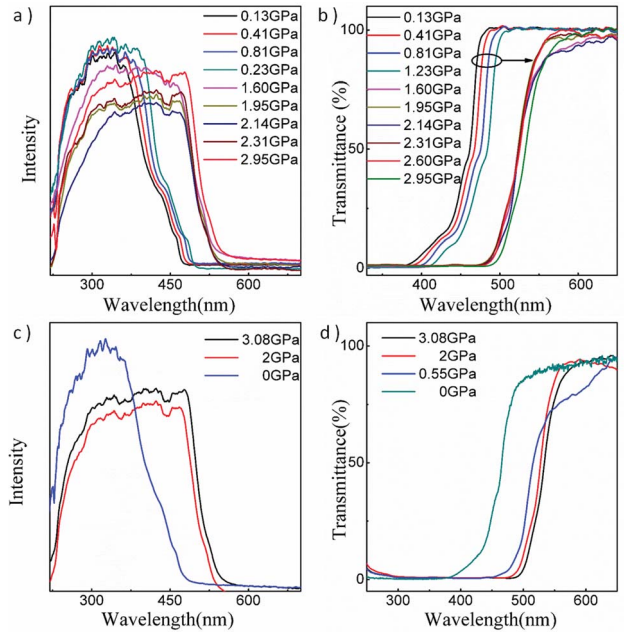

Fig. 9 (a) Absorption spectra of PBNA during the process of pressurization, (b) transmittance changes in the spectra of PBNA during the process of pressurization, (c) absorption spectra of PBNA during the process of depressurization, and (d) transmittance changes in the spectra of PBNA during the process of depressurization.

spectrum peak was at 639 cm^{-1}, and the peak location was displaced to 645 cm^{-1} after adding pressure. The spectrum peak returned to 639 cm^{-1} when the pressure was released, and this peak was the characteristic peak of deformation of a substituted benzene ring. Wave numbers of 826 cm^{-1} and 838 cm^{-1} in the Raman spectrum of the unpressurized crystal were the characteristic peaks of the ring vibration activity of a *para* disubstituted benzene, and these two wave numbers showed a displacement to 843 cm^{-1} and enhancement at the same time when the pressure was increased to 2.78 GPa, and returned back to the original values when the pressure was released. The wave numbers of 896 cm^{-1} and 885 cm^{-1} in the Raman spectrum of the unpressurized crystal were the characteristic peaks of the C–C stretching vibration. No significant changes occurred after the pressure was added (the peak positions were still located around 897 cm^{-1} and 889 cm^{-1}) thus indicating that the central axis of the PBNA molecule was unchanged on the whole, and not deflected or scalable during the pressing process. The intensity of the peak at 930 cm^{-1} in the Raman spectrum of the unpressurized crystal enhanced significantly but shifted very little to 932 cm^{-1} under pressure; this peak was attributed to the C–H curved peak changes. In the unpressurized spectrum, the peak at 960 cm^{-1} moved to 980 cm^{-1} and returned to 960 cm^{-1} on depressurizing, corresponding to the olefin C–H vibrations. The Raman spectrum changes also characterized the vibration of the benzene ring and the molecular plane. The unpressurised crystal Raman spectrum peak was around 1010 cm^{-1} and had a displacement of 10 cm^{-1}, and the intensity simultaneously enhanced during pressurization; the wave number position

Published on 29 Julai 2016. Downloaded by Fail Open on 23/07/2025 10:17:13.

represented the triangle ring "breathing" movement of the substituted benzene ring. The spectrum peak at 1022 cm^{-1} shifted to 1032 cm^{-1} and was accompanied by intensity enhancement during pressurization, returning to the original position during releasing pressure. The single peak at 1191 cm^{-1} changed to double peaks at 1193 cm^{-1} and 1204 cm^{-1}, and the emission intensity enhanced a lot; this could be attributed to the vibration between the benzene ring and carbon atom, and it returned to the single peak when the pressure was released. The shift from 1220 cm^{-1} and 1231 cm^{-1} to 1236 cm^{-1} and 1248 cm^{-1} was attributed to the vibration of *p*-substituted benzene during pressurization. The unpressurized Raman spectra had no peak at 1290 cm^{-1}, but at this location a new peak appeared as the pressure increased, and the peaks at 1327 cm^{-1} and 1347 cm^{-1} were also displaced to 1348 cm^{-1} and 1364 cm^{-1}; changes in these positions were attributed to C–H deformation vibrations. The shift of peaks from 1378 cm^{-1} and 1389 cm^{-1} to 1402 cm^{-1} and 1389 cm^{-1} were characterized as vibrations of the naphthalene ring, the same as the peak at 1410 cm^{-1}, and the previous emission intensity was clearly enhanced during pressurization.

New peaks at around 1449 cm^{-1} and 1483 cm^{-1} emerged as the pressure reached 1.4 GPa. The appearance of a peak at 1449 cm^{-1} represented a new interaction between a nitrogen atom and another nitrogen atom, and the peak at a wave number position of 1483 cm^{-1} was the symmetrical C=C stretching vibration. Peaks at around 1547 cm^{-1}, 1572 cm^{-1}, 1592 cm^{-1}, 1608 cm^{-1} and 1626 cm^{-1} shifted to 1551 cm^{-1}, 1597 cm^{-1}, 1596 cm^{-1}, 1621 cm^{-1} and 1642 cm^{-1}, respectively, and these peaks were the stretching movement of the carbon–carbon double bond during the pressurization process. The C≡N stretching activity was represented by a peak shift from 2227 cm^{-1} to 2241 cm^{-1}, accompanied by emission intensity enhancement on pressurization; these changes could return to their original state during depressurization. Finally, the characteristic benzene ring aromatic C–H stretching vibration was observed through the red shift from 3048 cm^{-1} and 3080 cm^{-1} to the 3083 cm^{-1} and 3109 cm^{-1} during pressurization.

The Raman spectra described the structural changes of the AIE molecule PBNA during the pressurization and depressurization process (Table 1), indicating that when the pressure exceeded 1.4 GPa, the phase had changed to a new one, producing new interactions between the molecules. A new peak appeared at 1449 cm^{-1} produced by the interaction of a nitrogen atom with another nitrogen atom, and the peak shape and intensity of the emission spectrum showed a mutation phenomenon synchronously. These phenomenon all demonstrated the molecules in crystal G being pressurized to become planar and then transformed into another phase. During depressurization, the molecules tended to be stretchable and returned back from the new phase to the original one.

The absorption spectra of the crystal were also measured and images of the transmittance changes during the process of pressurizing and depressurizing were constructed (Fig. 9). These two types of image illustrated the same phenomenon, but in the transmittance spectra the ratio value of transmitted light was observed intuitively. Fig. 9a shows that the maximum absorption wavelength position changed from 450 nm to 550 nm during pressurization. Fig. 9b shows that the start position at which light could transmit through also shifted from around 400 nm to 500 nm, and the wavelength of the light transmitted through changes from 480 nm to 580 nm. During the process of releasing the pressure, there still existed a reversible change.

 This journal is © The Royal Society of Chemistry 2017

Published on 29 Julai 2016. Downloaded by Fail Open on 23/07/2025 10:17:13.

Conclusions

Molecular structure changes during pressurization and then depressurization were studied by synchronous Raman scattering and fluorescence spectroscopies. The colour changes and spectroscopic changes during the process were observed and tested. From the spectra, a red-shift value of 142 nm of the emission spectrum peak of the PBNA crystal during pressurization was observed, which is larger than that of other reported AIE crystals, and the phase transformation process was revealed by the Raman spectra. The planar structure of the PBNA molecules made it easy for the crystal to be transformed to another phase when the pressure was increased above 1.03 GPa and for it to return to the original phase when the pressure was decreased to about 1.2 GPa. The combination of the synchronous Raman scattering with the phase transformation process was important in this paper to study the synchronous structure change of the single crystal. This special restorable piezochromic phase transformation phenomenon of the AIE crystal may aid the study of erasable optical information storage and stress sensing devices using AIE materials.

Acknowledgements

The authors express their thanks to the Natural Science Foundation of China (51303057, 21334002, 51573055, 51473052, 51521002, 51103054, 51273076, 91233113), the Ministry of Science and Technology of China (2013CB834705, 2015CB655003), the Fundamental Research Funds for the Central Universities, Introduced Innovative R&D Team of Guangdong (201101C0105067115), Major Science and Technology Project of Guangdong Province (2015B090913002), and Foundation of Guangzhou Science and Technology Project (201504010012) for their support.

Notes and references

1 J. Luo, Z. Xie, J. W. Lam, L. Cheng, H. Chen, C. Qiu, H. S. Kwok, X. Zhan, Y. Liu and D. Zhu, *Chem. Commun.*, 2001, **18**, 1740–1741.
2 Y. Hong, J. W. Lam and B. Z. Tang, *Chem. Commun.*, 2009, **29**, 4332–4353.
3 J. Chen, B. Xu, X. Ouyang, B. Z. Tang and Y. Cao, *J. Phys. Chem. A*, 2004, **108**, 7522–7526.
4 Z. Wang, H. Shao, J. Ye, L. Tang and P. Lu, *J. Phys. Chem. B*, 2005, **109**, 19627–19633.
5 B.-K. An, S.-K. Kwon, S.-D. Jung and S. Y. Park, *J. Am. Chem. Soc.*, 2002, **124**, 14410–14415.
6 S. J. Lim, B. K. An, S. D. Jung, M. Chung and S. Y. Park, *Angew. Chem., Int. Ed.*, 2004, **43**, 6346–6350.
7 W. Z. Yuan, P. Lu, S. Chen, J. W. Lam, Z. Wang, Y. Liu, H. S. Kwok, Y. Ma and B. Z. Tang, *Adv. Mater.*, 2010, **22**, 2159–2163.
8 W. Qin, D. Ding, J. Liu, W. Z. Yuan, Y. Hu, B. Liu and B. Z. Tang, *Adv. Funct. Mater.*, 2012, **22**, 771–779.
9 T. Han, X. Feng, B. Tong, J. Shi, L. Chen, J. Zhi and Y. Dong, *Chem. Commun.*, 2012, **48**, 416–418.

Published on 29 Julai 2016. Downloaded by Fail Open on 23/07/2025 10:17:13.

10 H. Li, X. Zhang, Z. Chi, B. Xu, W. Zhou, S. Liu, Y. Zhang and J. Xu, *Org. Lett.*, 2011, **13**, 556–559.
11 J. Huang, N. Sun, Y. Dong, R. Tang, P. Lu, P. Cai, Q. Li, D. Ma, J. Qin and Z. Li, *Adv. Funct. Mater.*, 2013, **23**, 2329–2337.
12 S. Choi, J. Bouffard and Y. Kim, *Chem. Sci.*, 2014, **5**, 751–755.
13 Y. Xu, K. Wang, Y. Zhang, Z. Xie, B. Zou and Y. Ma, *J. Mater. Chem. C*, 2016, **4**, 1257–1262.
14 Y. Yuan, R. T. Kwok, B. Z. Tang and B. Liu, *J. Am. Chem. Soc.*, 2014, **136**, 2546–2554.
15 X. Zhang, X. Zhang, S. Wang, M. Liu, Y. Zhang, L. Tao and Y. Wei, *ACS Appl. Mater. Interfaces*, 2013, **5**, 1943–1947.
16 M. Li, Y. Hong, Z. Wang, S. Chen, M. Gao, R. T. Kwok, W. Qin, J. W. Lam, Q. Zheng and B. Z. Tang, *Macromol. Rapid Commun.*, 2013, **34**, 767–771.
17 M. Li, J. W. Lam, F. Mahtab, S. Chen, W. Zhang, Y. Hong, J. Xiong, Q. Zheng and B. Z. Tang, *J. Mater. Chem. B*, 2013, **1**, 676–684.
18 X. Y. Shen, Y. J. Wang, E. Zhao, W. Z. Yuan, Y. Liu, P. Lu, A. Qin, Y. Ma, J. Z. Sun and B. Z. Tang, *J. Phys. Chem. C*, 2013, **117**, 7334–7347.
19 W. Z. Yuan, Y. Tan, Y. Gong, P. Lu, J. W. Lam, X. Y. Shen, C. Feng, H. H. Y. Sung, Y. Lu and I. D. Williams, *Adv. Mater.*, 2013, **25**, 2837–2843.
20 Y. Zhang, J. Sun, G. Zhuang, M. Ouyang, Z. Yu, F. Cao, G. Pan, P. Tang, C. Zhang and Y. Ma, *J. Mater. Chem. C*, 2014, **2**, 195–200.
21 C. Y. K. Chan, J. W. Y. Lam, Z. Zhao, C. Deng, S. Chen, P. Lu, H. H. Sung, H. S. Kwok, Y. Ma and I. D. Williams, *ChemPlusChem*, 2012, **77**, 949–958.
22 S.-J. Yoon, J. W. Chung, J. Gierschner, K. S. Kim, M.-G. Choi, D. Kim and S. Y. Park, *J. Am. Chem. Soc.*, 2010, **132**, 13675–13683.
23 J. Mei, J. Wang, A. Qin, H. Zhao, W. Yuan, Z. Zhao, H. Sung, C. Deng, S. Zhang and I. Williams, *J. Mater. Chem.*, 2012, **22**, 4290–4298.
24 Z. Song, R. Liu, Y. Li, H. Shi, J. Hu, X. Cai and H. Zhu, *J. Mater. Chem. C*, 2016, **4**, 2553–2559.
25 Y. Q. Dong, J. W. Lam and B. Z. Tang, *J. Phys. Chem. Lett.*, 2015, **6**, 3429–3436.
26 C. Feng, K. Wang, Y. Xu, L. Liu, B. Zou and P. Lu, *Chem. Commun.*, 2016, **52**, 3836–3839.
27 Y. Zhang, Q. Song, K. Wang, W. Mao, F. Cao, J. Sun, L. Zhan, Y. Lv, Y. Ma and B. Zou, *J. Mater. Chem. C*, 2015, **3**, 3049–3054.
28 Y. Zhang, J. Sun, G. Zhuang, M. Ouyang, Z. Yu, F. Cao, G. Pan, P. Tang, C. Zhang and Y. Ma, *J. Mater. Chem. C*, 2014, **2**, 4320–4327.
29 X. Han, Q. Bai, L. Yao, H. Liu, Y. Gao, J. Li, L. Liu, Y. Liu, X. Li, P. Lu and B. Yang, *Adv. Funct. Mater.*, 2015, **25**, 7521–7529.

 This journal is © The Royal Society of Chemistry 2017